Coordinated Management of Electrical Energy in a Steelworks and a Wind Farm

G. Alonso Orcajo, *Member, IEEE*, Josué Rodríguez D., José M. Cano, *Member, IEEE*, Joaquín G. Norniella, Francisco Pedrayes G., Carlos H. Rojas,

***Abstract*— This paper proposes a coordinated management of electrical energy in a steelworks and a wind farm that are connected to the same distribution network. The suggested solution seeks to improve the efficiency of the hot rolling mill, to reduce greenhouse gas emissions, to minimize the cost of the electrical energy utilized in the manufacture of steel coils, to increase the power system chargeability and to guarantee power quality. The proposal consists in constituting a virtual plant (comprising the wind farm and the rolling mill) to be managed by a single operator. The approach is mainly focused on the management of the virtual plant reactive power. The algorithm proposed to optimize this reactive power is based on the so-called particle swarm optimization. Three optimization strategies are analyzed: minimization of losses in the distribution network, minimization of the voltage deviation at two of its nodes, and maximization of the displacement factor in both the rolling mill and the wind farm. Losses are reduced by up to 15.5% when adopting the first strategy in comparison to the least efficient case. Voltage variations are kept at less than 1% at both nodes when using the second strategy, whereas deviations between 1 and 5% are obtained when implementing the other two strategies. The study is based on actual measurements and simulation tests.**

***Index Terms*— Hot rolling mill, particle swarm optimization, reactive power, steel, virtual plant, wind farm.**

I. INTRODUCTION

Improving the energy efficiency of industrial facilities, reducing their emissions of greenhouse gases and promoting the generation of electrical energy from primary sources of renewable origin are three of the major objectives set by the European Union for the coming years. These objectives must be met while maintaining the competitiveness of the facilities.

Steel plants and, more specifically, rolling mills are part of the electro-intensive industry. Metallurgical and steel factories came together in the 70s in Europe. Their high electric power demand forced these factories to be located close to large generation centers, where it was possible to obtain good prices per kWh and where thermoelectric power plants prevail nowadays, particularly those based on the use of coal.

G. Alonso Orcajo, José M. Cano, J. G. Norniella, F. Pedrayes and C. H. Rojas are with the Electrical Engineering Department, University of Oviedo, 33204 Gijón, Spain (e-mail: gonzalo@uniovi.es; jmcano@uniovi.es; jgnorniella@uniovi.es; pedrayesjoaquin@uniovi.es; chrojas@uniovi.es). Josué Rodríguez is with the Basque Country Research Centre of ArcelorMittal, Sestao Spain. (e-mail: josue.rodriguezdiez@arcelormittal.com).

The directives of the European Union about environmental matters and particularly in relation to greenhouse gas emissions will necessarily force the reconversion of both sectors in the immediate future. Coal thermal power plants will be required to incorporate desulfurization, denitrification and CO_2 capture systems into their production lines to avoid closure. As a matter of fact, various countries have already announced the closure of part of their coal-based plants in the short-term. Consequently, renewable generation is likely to be promoted to restore part of the dismantled power capacity. The already existent high-power transport networks, originally designed to cover thermoelectric generation, will favor the power restitution to a certain extent. However, the price per kWh might become more expensive under these circumstances, which could lead to the relocation of metallurgical and steel plants to countries with less demanding environmental directives and cheaper energy prices.

In order to consolidate the steel industry in the current production centers, it is necessary to design strategies aimed at reducing the costs of electric energy and at guaranteeing power quality while meeting the objectives in terms of energy and climate change or the profitability of the plants.

Exhorted by the EU [1], some steelmakers have started taking measures to reduce the emissions of CO_2 from their manufacturing plants over the coming decades. These measures are primarily aimed at curtailing the production of steel from coal-fired blast furnaces while simultaneously boosting that of direct reduced iron by using renewable energy sources such as green hydrogen. Moreover, the integration of renewable energy-based electricity generators into the plants and the increase in the use of scrap in electric arc furnaces are likewise contemplated, the target being to stimulate the consumption of electricity involving low or zero greenhouse gas emissions, e.g. that from solar or wind power sources. In this paper, a steelworks whose electric distribution network includes a wind farm is considered.

The opportunities offered by the coordinated operation of consumption and generation centers have been analyzed by other authors in the context of smart grids [2-4]. Such grids integrate energy consumption, storage and renewable-based generation systems. Virtual power plants are one of the clearest examples of a joint and coordinated operation of several agents with common interests, both technical and economic [5-9]. The efficient management of reactive power is one of the capabilities of these virtual plants, where different agents

collaborate by means of coordinated actions according to their rated powers and their particular operating conditions.

The algorithms for reactive power management and optimization in power systems are based on conventional and advanced procedures [10]. The former are based on linear [11] and non-linear programming. [12]. The latter can be based, for example, on neural networks [13], genetic algorithms [14] or heuristic and metaheuristic methods [15]. The particle swarm optimization (PSO) belongs to the group of metaheuristic methods [16-17]. In this paper, a widely used and suitable PSO-based algorithm is considered, as will be discussed. More specifically, this paper proposes the joint, coordinated and collaborative exploitation of a hot rolling mill (HRM) and a wind farm. The solution primarily seeks to improve the efficiency of the rolling mill, to reduce greenhouse gas emissions, to decrease the cost of electrical energy, to increase the power system chargeability and to guarantee power quality. The proposal consists in developing a virtual plant including the wind farm and the rolling mill. This virtual plant will be managed by an operator [18] that must meet the production objectives by observing the economic benefits that can be provided by the electricity market, the possible energy production according to weather forecasts and the services that can be offered to the distribution network. In order to promote this proposal, the electricity market operator could take such services into account in the daily management of the power system and, therefore, remunerate them in a regulated manner.

The virtual plant will be controlled by only one agent to buy and sell active power in agreement with the daily market in each supply zone, to program the daily rolling campaigns according to demand management criteria, to offer services related to reactive power injection, and to optimize the internal reactive power flows according to multiple-criteria target functions that can take into account parameters such as the reduction of distribution losses or the control of voltage stability and variations.

The rest of the paper is organized as follows. In Section II, the rolling mill plant and its associated distribution network are presented. The characteristics of the wind farm are briefly reported in Section III. Section IV describes several of the main objectives of the virtual plant. The reactive power management strategy and the objective functions that can be addressed by the optimization algorithm are included in section V. This algorithm, based on PSO, is described in Section VI. Several case studies are presented in Section VII. In Section VIII the proposal is validated, and the advantages are demonstrated. Finally, the conclusions of this study are gathered in Section VIII.

II. STEEL PLANT AND DISTRIBUTION NETWORK

The original HRM considered in this study is a classic plant built in the 80s and whose main electrical load is a roughing and finishing train. The roughing mill (RM) has two main drives (upper and lower). The finishing mill (FM) comprises six rolling stands. The drives are based on 12-pulse cycloconverters capable of controlling the synchronous motors that drive the rolls through a gear train. This topology also includes a passive filtering system to limit the injection of harmonics into the distribution network and to compensate for reactive power (Fig. 1).

The average electric energy consumption in the hot-rolling operation is between 70 and 80 kWh per ton of produced steel coil. Power quality is also of great importance because steel plants, as large consumers, can affect the distribution network greatly and are particularly sensitive to disturbances. Rolling mill campaigns involve 20-30 slabs per hour and approximately 470-530 slabs per day. Each slab can weigh up to 22-26 tons; therefore, the daily and annual demand in a HRM can reach up to 1 GWh and 365 GWh respectively, which is why proposals aimed at improving their energy efficiency offer a great opportunity for considerable savings [19].

In order to improve the reactive power management, a 15-MVA STATCOM is connected to the point of common coupling of the drives and the passive filtering system. The STATCOM is compatible with other future enhancements of the plant, including a renewal of the rolling stands based on technological advances.

A new stage of the plant renewal consists in the incorporation of a wind farm into the 132-kV distribution network that feeds the steel plant, including the rolling mill. The analyzed rolling campaigns are based on real records of an actual rolling mill. Figures 2 and 3 show the evolution of the active and reactive power demand of the hot rolling mill when ten slabs are rolled.

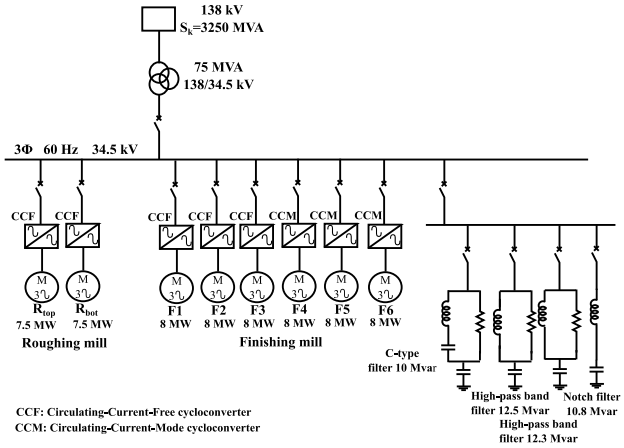

Fig. 1. Single-line diagram of the original plant.

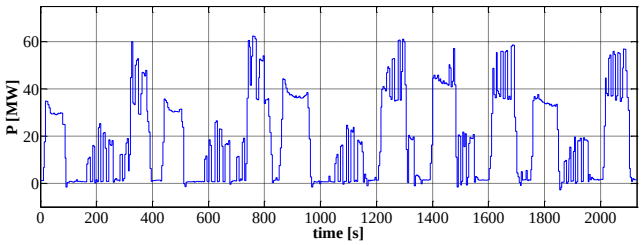

Fig. 2. Active power demand of the hot rolling mill.

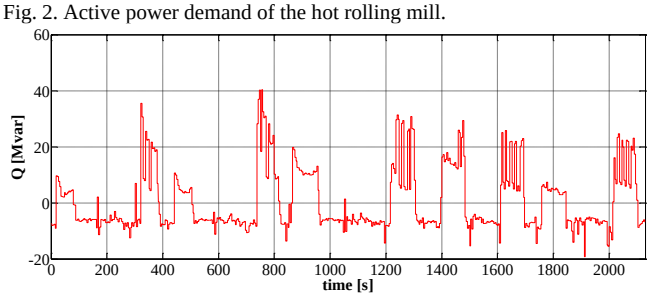

Fig. 3. Reactive power demand of the hot rolling mill.

The rolling mill, the wind farm and other installations that are part of the steel plant are connected to a 132-kV distribution network (Fig. 4). The power generation system consists of the wind farm and a 115-MVA plant for the recovery of the waste gases generated both in the blast furnaces during the pig iron production and in the coke batteries. This plant is based on synchronous generators driven by gas turbines. The consumption of the other installations of the steel plant is represented by their active and reactive power flows, which have been assumed to be constant (50 MW and 30 Mvar) in order to focus on the other consumption nodes. The 220-kV transmission network is connected to one of the nodes of the ring distribution grid by means of a 132/220 kV transformer.

TABLE I
TRANSFORMER PARAMETERS

Transformer	1-Wind	2-Steel	3-HRM	4-Wind	5-Slack
Sn [MVA]	20 x 1.75	75	75	47	200
U1/U2 [kV]	34.5/0.69	132/34.5	132/34.5	132/34.5	220/132
$\mathcal{E}_{Rcc}$; $\mathcal{E}_{Xcc}$ [%]	1; 5	1; 7.66	1; 7.66	0.53; 16	1; 15
Rm; Xm [pu]	500; inf	500; 500	500; 500	500; 500	500; 500

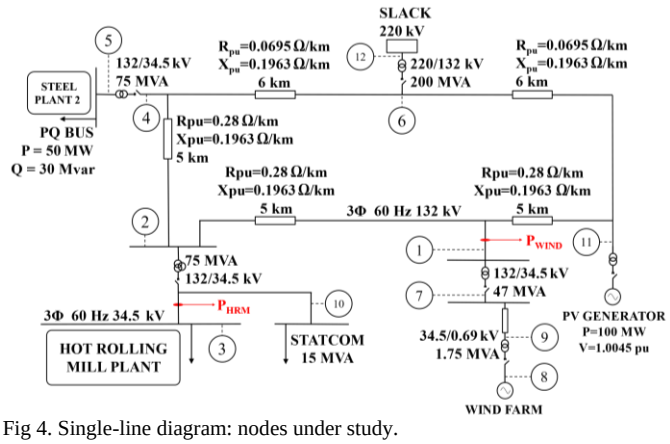

Fig 4. Single-line diagram: nodes under study.

III. WIND FARM

The planned wind farm consists of 20 wind turbines with a rated power of 1.5 MW each (i.e., a total installed capacity of 30 MW) and whose technical data are similar to those of commercial systems [20]. The turbines are based on a doubly fed induction generator (DFIG) able to control the active and reactive power flow. The average wind speed at the selected location is assumed to be 7.5 m / s at hub height (HH). Under these conditions and considering a cumulative Weibull distribution of wind duration, each turbine is assumed to generate up to 3.8 GWh / year, which means an annual production of the farm of $20 \cdot 3.8 = 76$ GWh (i.e., a capacity factor of 28.9 %). This amount of energy, coming exclusively from renewable sources, would cover 20.8 % of the annual demand of the rolling mill. The wind farm provides the plant with active energy generated with low greenhouse gas emissions (GHG) and conditioned by the daily wind speed profile. For a large part of its period of operation, the farm can utilize a reserve to supply capacitive or inductive reactive power depending on the needs.

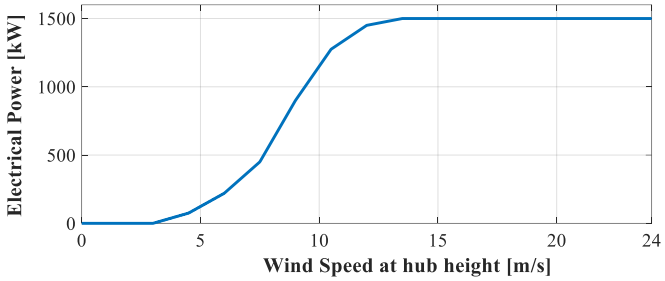

Fig. 5. Wind turbine power curve.

That reserve can be provided partly by the stator of the induction generator and partly by the converter connected to the network. The grid side converter (GSC), which normally manages between 20 and 30 % of the nominal power of the wind turbine, can be oversized for the power reserve to be greater. This reserve can be used to control the reactive power and also the injection of harmonics, the GSC thus playing the role of an active filter [21-22].

At present, a number of wind farms exist either nearby or on the grounds of various steelworks. The coordinated operation of the farm and the steelworks enables collaborative agreements [23].

IV. VIRTUAL PLANT

The main targets of the virtual plant are as follows:

- Coordinated management of the energy demand.
- Significant reduction of GHG emissions.
- Lessening of energy dependence.
- Improvement in the voltage profile.
- Decrease in losses.
- Control of reactive power.
- Voltage stability.
- Control of harmonics.
- Enhancement of the response under voltage sags.
- Improvement in the power network reliability.

A. Coordinated management of electrical demand.

The electric power production of the wind farm depends mainly on the average wind velocity and the power-speed curve of its turbines. This production can cover part of the demand of the rolling plant, thus reducing the active power distributed by the 132-kV network, the voltage drop at the PCC and the losses upstream this point.

The average wind speed determines the active power production of the farm and depends, among many other factors, on the local time and season. There are various applications that enable a reliable forecast of the hourly average wind speed between 8 and 10 hours in advance [24]. The power produced by a wind farm along with the average daily wind speed is exampled in Fig. 6. As can be seen, the farm operates at rated power (30 MW) between 13:00 and 14:00, while barely 1 MW are supplied from 9:00 to 10:00.

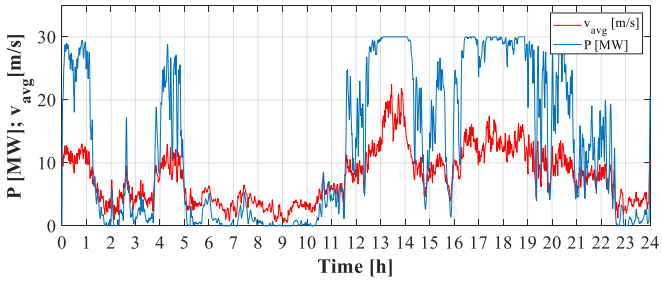

Fig. 6. Average wind speed at 80 m height. Data provided by the National Renewable Energy Laboratory. Date: 03/02/2021 [25].

Assuming that the wind farm generates 10 MW under a capacity factor of 0.333 (0.5 MW per turbine, 20 generators), a comparison of the power demanded by the installation in presence or absence of the wind farm can be seen in Fig. 7. The difference in the energy demanded by the installation under the two operating conditions is 1,761 kWh over the 550 s considered rolling profile. The positive impact of the joint operation of the HRM and the wind farm on the active energy consumption is evident.

The rolling campaigns can be organized seeking for the simultaneity of the generation of energy by the wind farm and the demand of active power while honoring the production criteria of the plant.

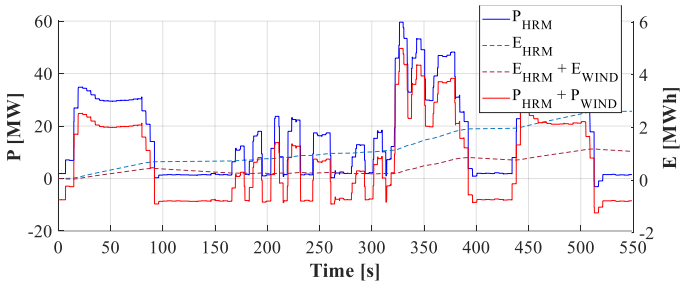

Fig. 7. Active power and energy demand in presence or absence of the wind farm.

B. Emissions of greenhouse gases

The CO_2 emissions per kWh are a function of the primary source used by the generation power station. Accordingly, 0.961 kg of CO_2 per kWh are emitted by a coal thermal plant; 0.651 kg of CO_2 per kWh by ~~a~~ fuel-gas plant; 0.372 kg of CO_2 per kWh by ~~a~~ combined-cycle natural gas plant, and 0.006 kg of CO_2 per kWh by a wind farm. The emissions of the Spanish electricity mix were estimated at 0.341 kg of CO_2 per kWh in 2018 [26].

The expected reduction in CO_2 emissions in incorporating the wind farm is 21,142 ton per year when compared to the emissions from the energy mix, and 59,582 ton per year with respect to those from a generation system solely based on coal thermal power plants.

C. Control of wind farm reactive power

The capability of the wind farm to control the reactive power is determined by that of its turbines [27-28]. Accordingly, the reactive power manageable by the DFIG stator depends on both the active power transferred to the grid and the rated current of the stator itself. It also depends on the rotor rated current and voltage, given that the stator injection of active and reactive power is controlled through the d-q components of the rotor current. This control depends, in turn, on the voltage applied by the converter connected to the rotor. Moreover, the injection of reactive power from the GSC is limited by both the rated power of the converter itself and the active power transferred to the grid by the rotor.

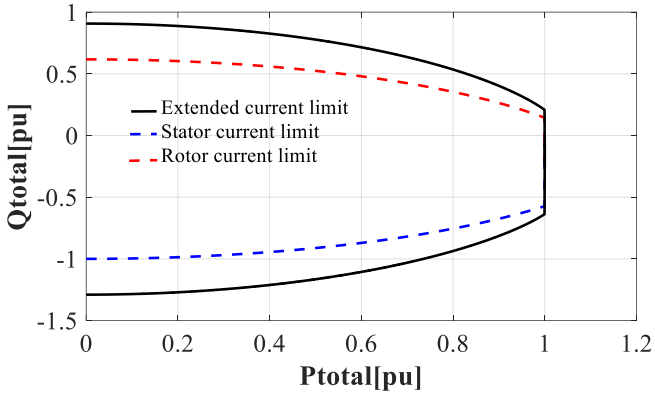

Fig 8. Reactive power injection limits according to active power supply.

Previous works have concluded that the limiting variable as for the injection of reactive power from the DFIG is normally the rotor current whereas the stator current is that for the reactive power demand. The rotor voltage only has influence at high slips. Figure 8 proves these statements correct by showing the power injection capability of the analyzed wind turbines. The injection of reactive power from the wind farm enables the fulfillment of the network operator needs as for the control of the PCC voltage and the virtual plant displacement factor, as well as for the support against potential voltage sags while avoiding the overload of the wind turbines and the shutdown of the rolling stands.

V. REACTIVE POWER MANAGEMENT SYSTEM

Reactive power management was mainly handled by large generators in traditional power systems. Nowadays, the increasing proliferation of distributed generation offers the opportunity to decentralize both the active and the reactive power management. In the specific context of industrial production plants, the incorporation of distributed generation systems can improve their operating conditions and bring economic benefits. As for the former, voltage variations at the PCC are controlled, as is the reactive power, which reduces losses and the loading of lines, transformers and protections, and gives support to overcome voltage sags without leading to interruptions in production cycles. As for the latter, the transmission system operator offers a reactive power injection/consumption service able to bring economic benefits to the plant.

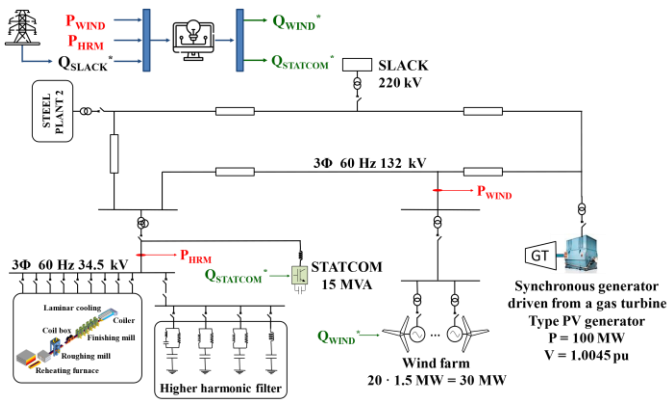

Fig. 9. Diagram of the ring distribution network under study.

One of the main objectives of our approach is to ensure that the HRM and the wind farm are managed collaboratively and jointly. Once the strategies for managing the active power demand are set, attention must be paid to the optimal management of reactive power. In this case, the goal is to define the most suitable optimization algorithm to set, in real time, the reactive power references for the wind farm generators and the STATCOM connected at the PCC. These references are strongly influenced by the technical constraints of the equipment (wind conditions, nominal power of the wind turbines and the STATCOM, etc.). Moreover, they also depend on the operating conditions of the grid, i.e. the reactive power setpoint at the PCC according to the system operator directives, the existing regulations, and the technical constraints of the distribution grid itself (line current limitations, protections response, voltage stability and variation, etc.). In general, the presence of numerous dispatchable units guarantees that there are sufficient degrees of freedom to meet the network optimization objectives once the above restrictions are met. This optimization process can address individual objectives or several targets by weighing them appropriately in multi-objective functions, among which the following are assessed:

1. Minimization of losses in the distribution network. This objective involves minimizing the following function:

$$P_{losses} = \sum_k G_k(i,j)\left[V_i^2 + V_j^2 - 2V_iV_j\cos(\delta_i - \delta_j)\right] \quad (1)$$

where V_i (and V_j) and δ_i (and δ_j) represent, respectively, the modulus and phase of the voltage at node i (and j), and G_k, the conductance of line k (connecting nodes i and j).

2. Minimization of the penalty for power factors beyond the admissible range. Spanish regulations concerning energy production from renewable sources set a mandatory power factor between 0.98 capacitive and 0.98 inductive at the PCC [26]. These guidelines may be temporarily modified by the system operator according to the needs of the network and may even respond to the tracking of a voltage reference at a specific node [29].
3. Minimization of the voltage deviation at the nodes of the internal network of the virtual plant, which is usually expressed through factor $VD = \sum_i |V_i - V_i^*|$, where V_i^* is the voltage assigned to node i. The participation in the transmission grid voltage control is remunerated in accordance with the existing guidelines in each country. In Spain, the system operator gives generators in charge of controlling node voltages priority for dispatching purposes, which also provides an economic benefit.

VI. PARTICLE SWARM OPTIMIZATION

Although reactive power optimization problems are nowadays profusely studied in the literature, our approach aims at responding to several challenges that arise in the application under study. For instance, these optimization problems are solved in minutes by using traditional systems in public distribution networks; however, the reactive power references sent to the various dispatchable elements in the virtual plant must be updated in a few seconds to maximize the positive impact of this solution. Therefore, heuristic methods (which, although quasi-optimal, are extremely robust) are utilized.

The specific method to be used is the so-called PSO [30-32]. The PSO is a metaheuristic optimization strategy based on populations and aimed at finding global minima or maxima. More specifically, population-based metaheuristic methods consist in calculating the trajectory followed by a population of individuals at each iteration to find a quasi-optimal solution from the evolution of a set of points in space. These methods are inspired by the behavior of flocks of birds, schools of fish or swarms of insects, in which the movement of each individual as for direction, speed, acceleration, etc. is the result of combining their particular decisions and the conduct of the rest. PSO algorithms aimed at maximizing or minimizing a function with one or multiple variables usually take the following steps: a) creation of an initial swarm of n random particles; b) evaluation of the objective function for each particle; c) calculation of the movement of each particle and subsequent update of their position and velocity; d) verification of stopping conditions and, if not met, return to step b). The proposed PSO-based algorithm consists of the following specific steps:

- Step 1: Voltages required at each node are set.

- Step 2: Restrictions on the reactive power injected/absorbed by the wind farm and the STATCOM are fixed according to the particular operating conditions.

- Step 3: The most representative impedances of transformers and distribution network lines are identified.

- Step 4: Elements of the admittance, susceptance and conductance matrices are calculated.

- Step 5: Characteristic power values at the PQ buses and the PV bus are identified. Net injected power values are calculated.

- Step 6: The PSO-based optimization algorithm is run. The utilized number of particles (Np) is 50 and the expected iterations are 150. The optimization is conducted by acting on two variables, namely the reactive power managed by the wind farm and that handled by the STATCOM. Limits to the position of the particles are defined: in the case of the wind farm, according to the generated active power; in the case of the STATCOM, with regard to its nominal power (15 MVA). Inertia weight, w = 0.729, cognitive weight, $c1$ = 1.49445, and social weight, $c2$ = 1.49445, are defined.

- Step 7: Several matrices are defined: particle swarm position, particle velocity, best positions, best values of each particle, Jacobian, and global best values.

- Step 8: Reactive power values are assigned to nodes 8 and 10 (see Fig. 4) according to the position of the corresponding particle.

- Step 9: The load flow is solved by using the Newton Raphson's method for the modulus and argument of the node voltages to be calculated. First, the node voltages are initialized at 1 pu and 0 rad. The voltage at the PV node is set to 1.0045 pu. Secondly, the reactive power at the slack bus and at the PV node is obtained to calculate the Jacobian matrix. Thirdly, extended submatrices H, L, M and N are calculated. Fourthly, power mismatches (dP and dQ) are calculated and compared with a power flow convergence threshold of 10^{-6}. When both

power mismatches are lower than this threshold, the Newton-Raphson's algorithm is stopped.

- Step 10: Different cost functions are evaluated depending on the selected objective. Therefore, cost functions associated with 1) losses in the distribution network, 2) the displacement factor at the PCC of the wind farm and the HRM or 3) voltage variations at nodes 3 and 8 are assessed. In all cases, the discrepancy between the reactive power injected into the slack bus and that set as a reference is calculated. Penalties are included in such functions if the particle is beyond the maximum and minimum limits. The best particle swarm solution is recorded at each iteration. An analysis of the results of the Np particles at the current iteration is conducted. The best results for each particle and for the whole swarm are stored.

- Step 11*:* The particle position and speed are updated.

- Step 12*:* The best reactive power references for the wind farm generators and the STATCOM are obtained after iterating for the Np particles.

The virtual plant is simulated by using general-purpose software for analyzing electrical power systems [33]. The simulations enable the verification of the fulfillment of the objectives pursued with the incorporation of the PSO strategy. The algorithm input data (active and reactive power of the HRM and active power of the wind farm) and the STATCOM and farm reactive power references are updated every 10 ms. A sample time of 5 μs is used.

VII. CASE STUDIES

Three case studies corresponding to the objectives described in Section V are analyzed, namely the minimization of distribution losses (case A), the maximization of the displacement factor at the 132-kV PCC of the HRM (PCC_B1; node 2) and the wind farm (PCC_B2; node 1) (case B), and the minimization of the voltage deviation at both the 690-V PCC (PCC_C1; node 8) of the turbines and the 34.5-kV PCC (PCC_C2; node 3) of the HRM (case C). The input variables of the algorithm are the active and reactive power demanded by the HRM, as well as the active power produced by the wind farm, for each case study and optimization interval. The active power generated by the waste gas recovery plant is 100 MW and its associated node voltage is 1.0045 pu. Plant 2 behaves as a PQ load (P = 50 MW and Q = 30 Mvar).

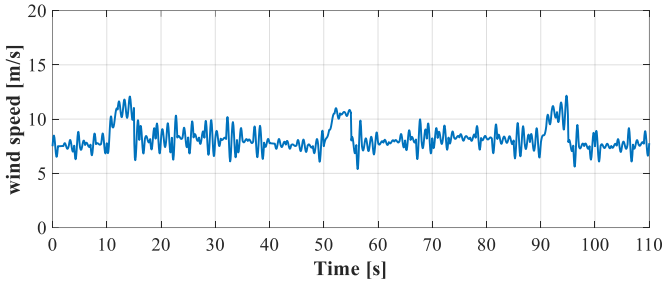

Fig. 10. Wind speed evolution over time.

The expected wind speed distribution during the analysis is shown in Fig. 10. This distribution comprises four fundamental components: base wind, which corresponds to the average wind speed (7.5 m / s); gust, which represents sudden wind changes; gradual wind changes, and wind of random nature. The reactive power reference of the slack bus in cases A and C is assumed to keep constant (1.5 Mvar) according to that set by the transmission grid manager, whereas such a reference cannot be set in case B. The algorithm provides the references for the reactive power injected by the STATCOM and the wind farm. The evolution of the main variables of interest when the slab is rolled in the FM is shown in Figs. 11 (case A), 12 (case B), and 13 (case C). Figure 14 shows the evolution of the distribution losses for each case study (LS: minimization of losses; DF: maximization of displacement factor; AU: minimization of voltage deviation). As can be seen, the maximum difference (roughly 400 kW) occurs between cases A (2 MW) and B (2.4 MW) when the FM is loaded.

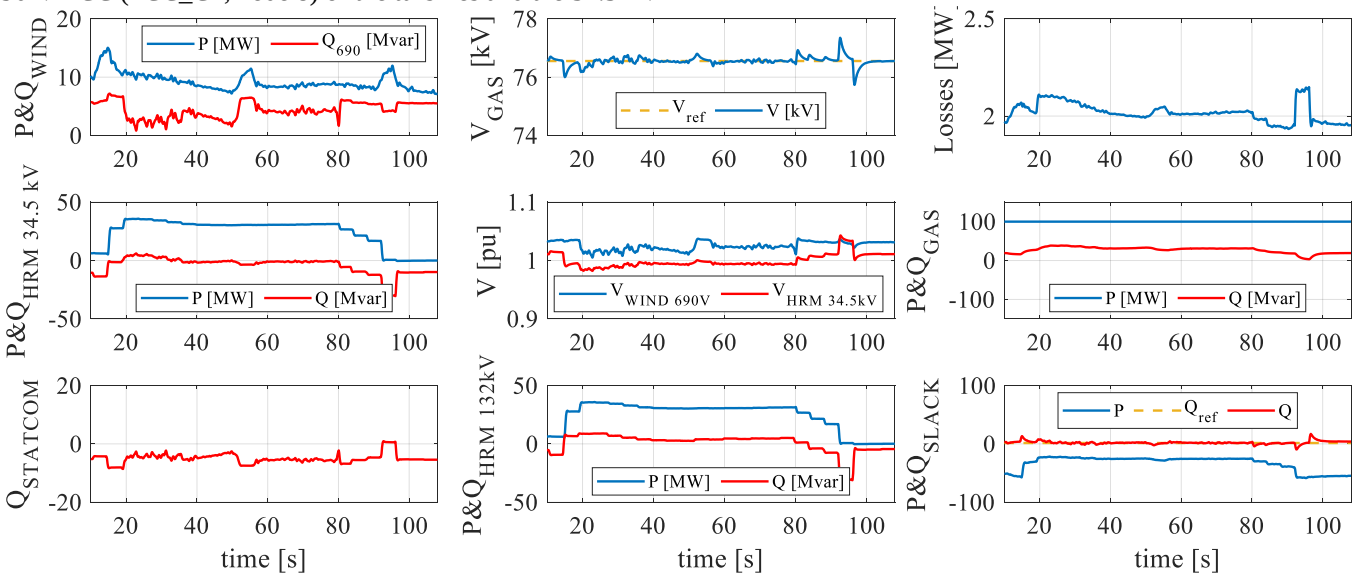

Fig. 11. Case A when a slab is rolled in the FM. From left to right and from top to bottom: 1) Active (blue) and reactive (red) power injected by the wind farm. 2) Reference (yellow) and measured (blue) voltage at the PV node of the gas-based power plant. 3) Power losses in the ring distribution network under study. 4) Active (blue) and reactive (red) power demanded from the HRM downstream the STATCOM PCC. 5) Voltage at PCC_C1 (blue) and PCC_C2 (red). 6) Active (blue) and reactive (red) power injected by the gas-based power plant. 7) Reactive power absorbed by the STATCOM. 8) Active (blue) and reactive (red) power demanded by the HRM at PCC_B1(node 2). 9) Active (blue) and reactive power (red) demanded by the 220 kV network at the slack bus, and reactive power reference (yellow) for the optimization algorithm.

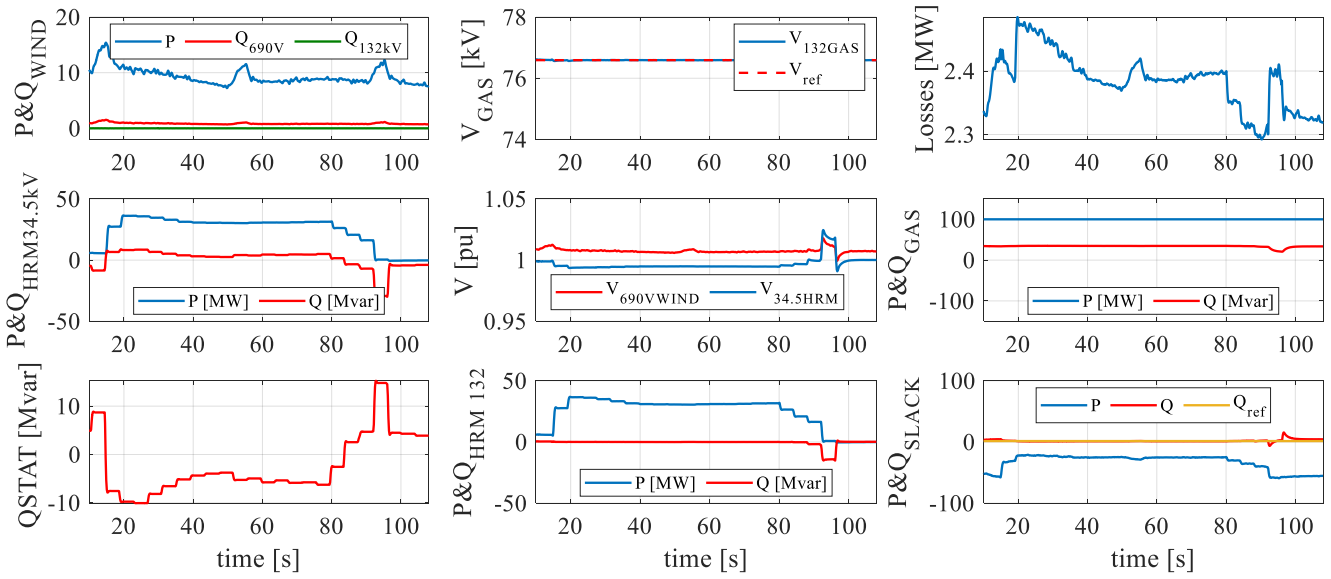

Fig. 12. Case B when a slab is rolled in the FM. From left to right and from top to bottom: 1) Active (blue) and reactive (red) power injected by the wind farm, and reactive power (green) at PCC_B2 (node 1). 2) Reference (yellow) and measured (blue) voltage at the PV node of the gas-based power plant. 3) Power losses in the ring distribution network under study. 4) Active (blue) and reactive (red) power demanded from the HRM downstream the STATCOM PCC. 5) Voltage at PCC_C1 (blue) and PCC_C2 (red). 6) Active (blue) and reactive (red) power injected by the gas-based power plant. 7) Reactive power absorbed by the STATCOM. 8) Active (blue) and reactive (red) power demanded by the HRM at PCC_B1(node 2). 9) Active (blue) and reactive power (red) demanded by the 220 kV network at the slack bus, and reactive power reference (yellow) for the optimization algorithm.

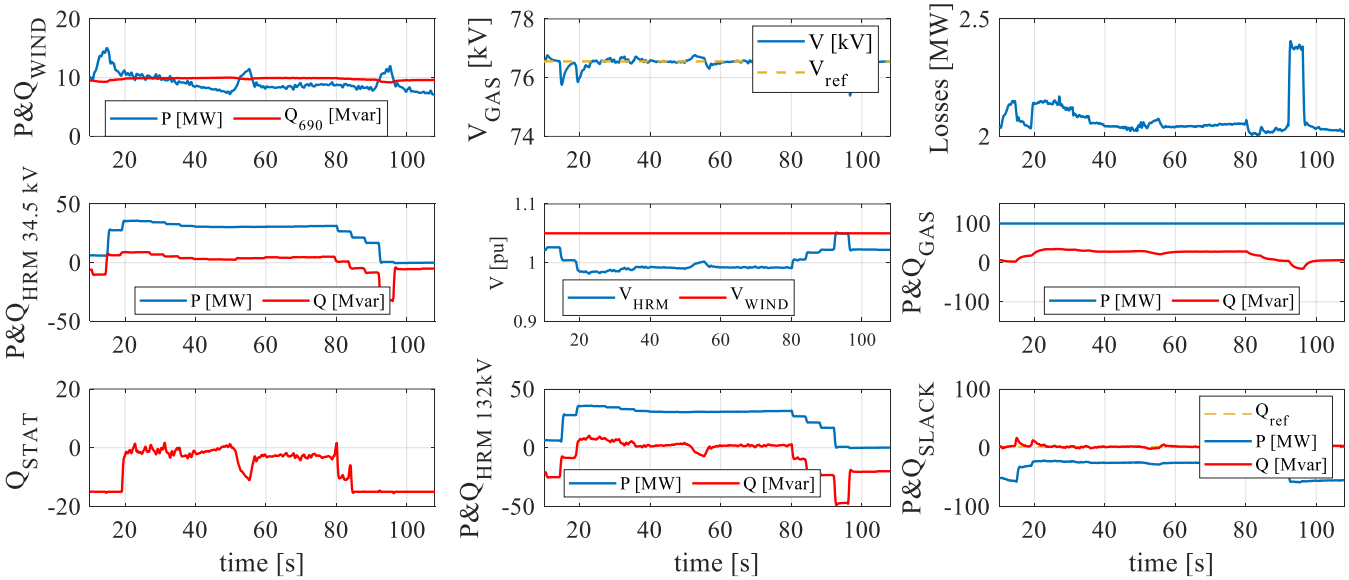

Fig. 13. Case C when a slab is rolled in the FM. From left to right and from top to bottom: 1) Active (blue) and reactive (red) power injected by the wind. 2) Reference (yellow) and measured (blue) voltage at the PV node of the gas-based power plant. 3) Power losses in the ring distribution network under study. 4) Active (blue) and reactive (red) power demanded from the HRM downstream the STATCOM PCC. 5) Voltage at PCC_C1 (blue) and PCC_C2 (red). 6) Active (blue) and reactive (red) power injected by the gas-based power plant. 7) Reactive power absorbed by the STATCOM. 8) Active (blue) and reactive (red) power demanded by the HRM at PCC_B1(node 2). 9) Active (blue) and reactive power (red) demanded by the 220 kV network at the slack bus, and reactive power reference (yellow) for the optimization algorithm.

On another note, the iron losses of the network transformers are expected to be 864 kW. These losses can be considered practically constant given the small variation observed in the voltage of the transformers PCC. Therefore, 400 kW in case A represent 26% of the total losses that can be controlled (2.4 MW – 864 kW = 1.536 MW), which is a significant benefit.

With regard to the voltage at PCC_C1 and PCC_C2, their optimum references are set to 1 and 1.05 pu respectively (note that these references do not have necessarily to be 1 pu). Voltage variations with respect to the optimum value are always of the order of 1 % (when the algorithm optimizes voltage variations) or up to 5 % (when distribution losses are minimized).

The evolution of the main variables of interest when one slab is rolled in the RM is shown in Fig. 15 (cases A, B, and C). On the other hand, the evolution of the same variables when two slabs are rolled simultaneously, one in the RM and the other in the FM, is plotted in Fig. 16 (cases A, B, and C). The analysis of the results obtained for these two rolling circumstances and under the three optimization algorithms is performed by comparing the distribution network losses (Fig.

17) and the voltage variations (Fig. 18) at the monitored nodes, PCC_C1 (corresponding to the wind farm, WF and PCC_C2 (associated with the HRM). Figure 19 summarizes the losses and voltage deviations for each of the three algorithms, three rolling circumstances and two monitored nodes. More specifically, the maximum voltage deviation that occurs is indicated for each case.

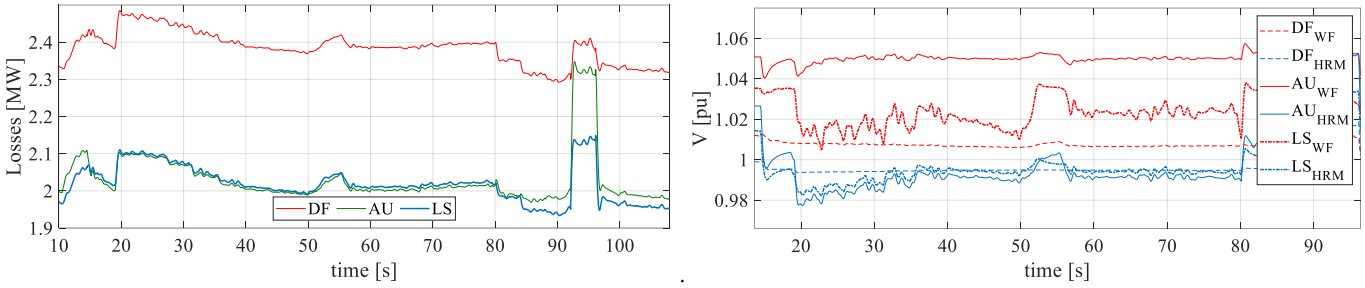

Fig. 14. Evolution of losses (left) and of the voltage at PCC_C1 and PCC_C2 (right) for the three optimization algorithms.

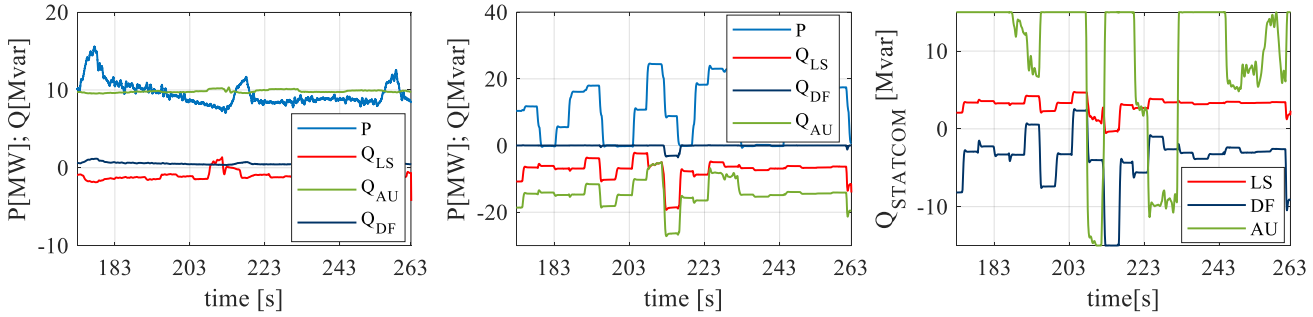

Fig. 15. Cases A, B and C when a slab is rolled in the RM. From left to right: 1) Active (blue) and reactive (red, green, dark blue) power injected by the wind farm. 2) Active (blue) and reactive (red, green, dark blue) power demanded by the HRM at PCC_B1(node 2). 3) Reactive power injected by the STATCOM.

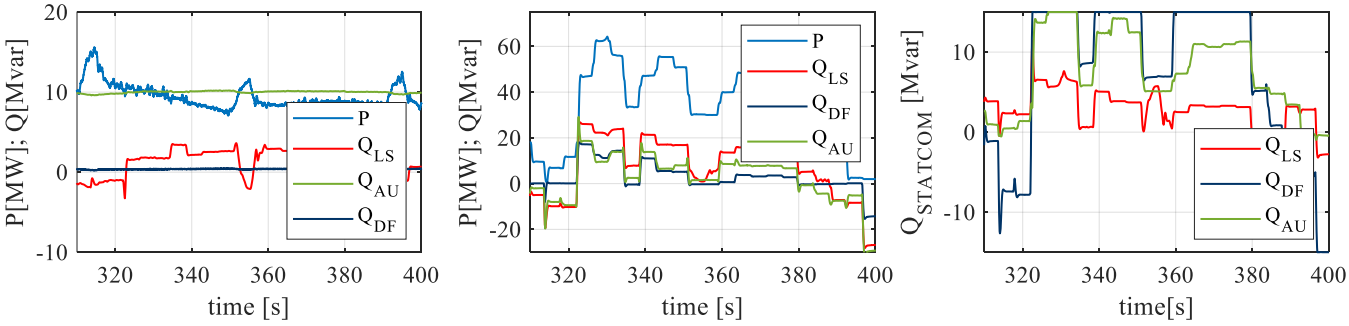

Fig. 16. Cases A, B and C when two slabs are rolled simultaneously in the RM and the FM. From left to right: 1) Active (blue) and reactive (red, green, dark blue) power injected by the wind farm. 2) Active (blue) and reactive (red, green, dark blue) power demanded by the HRM at PCC_B1(node 2). 3) Reactive power injected by the STATCOM.

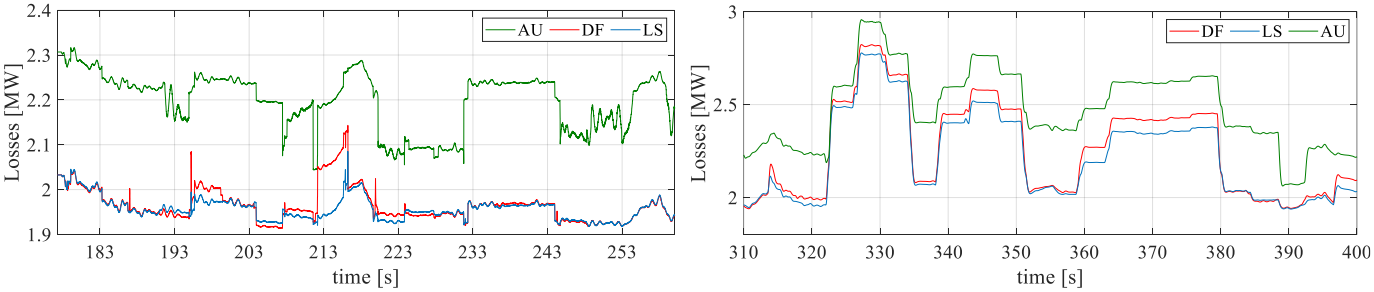

Fig. 17. Evolution of losses when a slab is rolled in the RM (left) and when two slabs are rolled simultaneously in the RM and the FM (right) for each optimization algorithm.

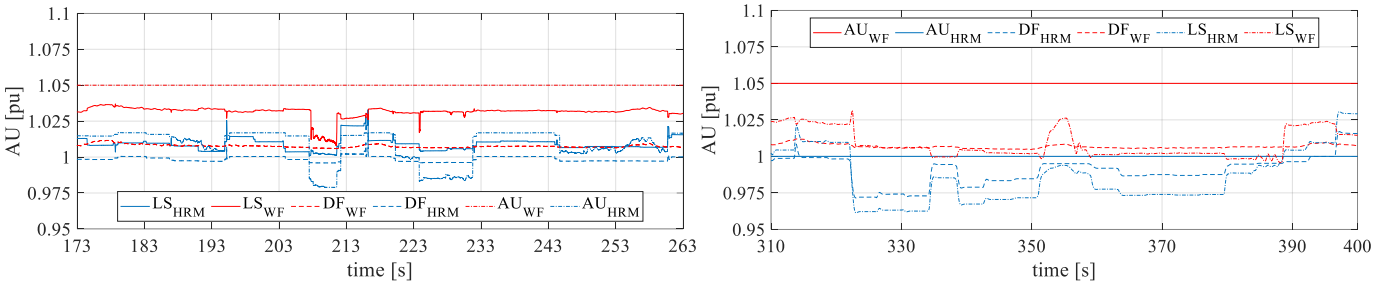

Fig. 18. Evolution of voltage deviation when a slab is rolled in the RM (left) and when two slabs are rolled simultaneously in the RM and the FM (right) for each optimization algorithm.

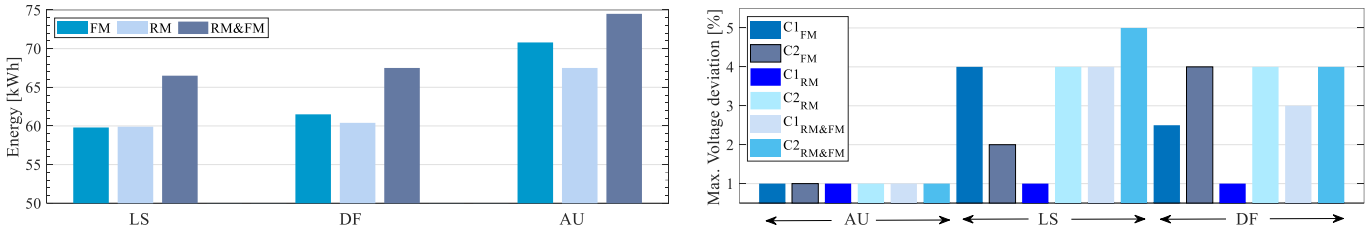

Fig. 19. Comparative analysis of energy losses (left) and voltage deviation at PCC_C1 and PCC_C2 (right) for the three optimization strategies (LS, DF and AU) when a slab is rolled in the FM or in the RM, and when two slabs are rolled simultaneously in the RM and in the FM.

Losses are reduced by 11-15.5% when adopting the losses minimization strategy in comparison to the least efficient case, as seen in Fig. 19 (left). An average saving of 130 kWh is achieved when rolling 10 slabs if such a strategy is employed, which yields savings of 6.5 MWh per day and 2.3 GWh per year assuming a daily rolling rate of 500 slabs. Voltage variations are maintained at less than 1% at both nodes when employing the strategy for minimizing voltage deviations, whereas fluctuations between 1.5 and 5% are reached when implementing the other two strategies, as seen in Fig. 19 (right).

The displacement factor is kept close to unity at nodes 1 and 2 if the strategy for maximizing the displacement factor is selected. On the contrary, the displacement factor at these nodes can reach notably poor values when the other strategies are adopted, especially at node 2 and under low load conditions.

VIII. VALIDATION OF RESULTS

The utilized PSO algorithm is able to give a response within an optimal range in a reasonably short time (10 ms), which perfectly suits the demanding dynamics of the steel plant. Moreover, the computational cost associated with this algorithm is low. Furthermore, its flexibility is greater than that of more reliable and robust linear programming-based methods, thus making it able to work with both linear systems and non-linearities such as those associated with the responses produced by the wind farm and the STATCOM themselves. Although optimization strategies based on genetic algorithms also deliver good performance under non-linear constraints, their computational cost is higher [34]. The main disadvantage of the PSO technique is the impossibility of analyzing the a priori quality of the obtained quasi-optimal solution; however, it is possible to determine whether the solution pertains to an optimal range or not in the considered case studies. The quality of the solution is particularly simple to assess when optimizing the displacement factor or minimizing the voltage variations. In these cases, a small margin for improvement can be observed. If the target is the minimization of losses, the upper and lower limits make it possible to verify that the solution is within the optimal range, the former limit being obtained when other objectives are pursued, and the latter being set by the no-load transformer losses.

The results obtained by applying the PSO algorithm have been compared with those yielded by the Matlab® function called *fmincon* [34-35]. This function is an interior-point optimization algorithm and a nonlinear programming solver. In particular, the comparison is made when the LS algorithm is selected, as is the case for which the validity of the results can be more uncertain. Figure 20 shows the evolution of the main input variables, which are the same for both the PSO algorithm and the *fmincon* function, as is the slack bus reactive power reference (1.5 Mvar). Figure 21 shows the evolution of the primary output control variables, i.e. the reactive power references for the wind farm and the STATCOM. The accordance between the results yielded by both methods can be noticed. Meanwhile, Fig. 22 shows the evolution of the distribution network losses when calculated with each of the optimization methods. The total agreement of the results can be observed. The question then arises as to why use the PSO-based algorithm instead of the *fmincon* function.

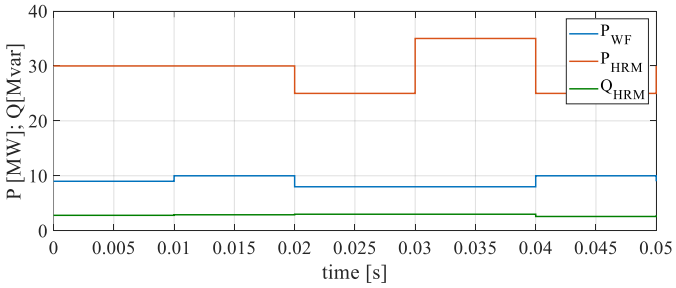

Fig 20. Evolution of the main input variables during the comparative analysis.

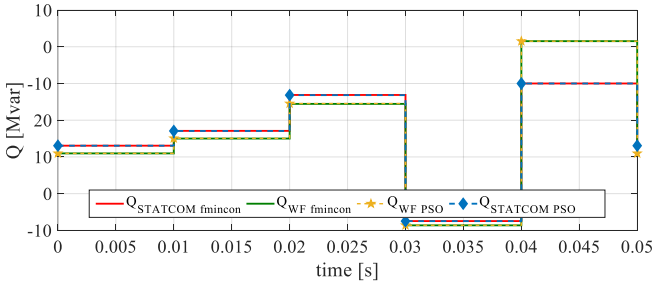

Fig 21. Evolution of the main output control variables during the comparative analysis

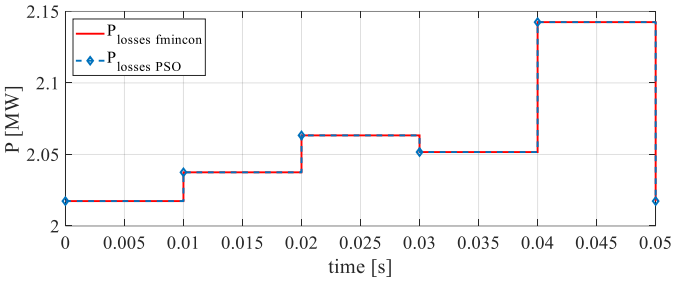

Fig 22. Evolution of the distribution losses during the comparative analysis.

The main advantages of the PSO algorithm when compared to the *fmincon* function are as follows: 1) separate cores of the same computer can be used to run different particles of the PSO technique simultaneously, which renders this technique much faster; 2) the PSO algorithm is more flexible than the Matlab function, and 3) the PSO technique supports different minimization targets that can be weighted and processed in parallel, whereas the initial value defined for *fmincon* can lead to a difficult convergence for the Newton-Raphson algorithm, the obtained solution thus possibly being a local minimum.

IX. CONCLUSION

The opportunities offered by a collaborative operation of steel plants and power generation centers have been analyzed in this paper. The specific proposal consists in integrating a wind farm and a steelmaking factory into a virtual plant managed by a single operator. Special attention has been paid to the optimal management of reactive power, which has been solved by using the so-called particle swarm optimization. This method can address different objective functions. Accordingly, optimization of losses, of two node voltages and of the displacement factor have been assessed. The obtained results demonstrate the advantages of the coordinated management of energy and the effectiveness of the utilized optimization algorithm.

ACKNOWLEDGMENTS

The authors gratefully acknowledge the Research and Development Center of ArcelorMittal (Spain) and the Ministry of Economy and Competitiveness of Spain (project within the framework of the National Plan of Research, Development and Innovation, reference DPI2017-89186-R), for their technical and financial support during this study.

REFERENCES

[1] European Union publications. Commission Staff working document “Towards competitive and clean European steel” Brussels, 5.5.2021 SWD (2021) 353 final. 2021

[2] F. Delfino, G. Ferro, M. Robba and M. Rossi, "An Energy Management Platform for the Optimal Control of Active and Reactive Powers in Sustainable Microgrids," in IEEE Transactions on Industry Applications, vol. 55, no. 6, pp. 7146-7156, Nov.-Dec. 2019, doi: 10.1109/TIA.2019.2913532.

[3] R. Zhang and B. Hredzak, "Distributed Dynamic Clustering Algorithm for Formation of Heterogeneous Virtual Power Plants Based on Power Requirements," in IEEE Transactions on Smart Grid, vol. 12, no. 1, pp. 192-204, Jan. 2021, doi: 10.1109/TSG.2020.3020163.

[4] Z. Tan, H. Zhong, Q. Xia, C. Kang, X. S. Wang and H. Tang, "Estimating the Robust P-Q Capability of a Technical Virtual Power Plant Under Uncertainties," in IEEE Transactions on Power Systems, vol. 35, no. 6, pp. 4285-4296, Nov. 2020, doi: 10.1109/TPWRS.2020.2988069.

[5] J. García-González, J. L. Luis Mata and R. Veguillas, "Improving the integration of renewable sources in the European electricity networks," *IEEE PES General Meeting*, Minneapolis, MN, USA, 2010, pp. 1-2, doi: 10.1109/PES.2010.5589567.

[6] A. Mnatsakanyan and S. W. Kennedy, "A Novel Demand Response Model with an Application for a Virtual Power Plant," in IEEE Transactions on Smart Grid, vol. 6, no. 1, pp. 230-237, Jan. 2015

[7] A. Thavlov and H. W. Bindner, "Utilization of Flexible Demand in a Virtual Power Plant Set-Up," in IEEE Transactions on Smart Grid, vol. 6, no. 2, pp. 640-647, March 2015, doi: 10.1109/TSG.2014.2363498.

[8] M. Vasirani, R. Kota, R. L. G. Cavalcante, S. Ossowski and N. R. Jennings, "An Agent-Based Approach to Virtual Power Plants of Wind Power Generators and Electric Vehicles," in IEEE Transactions on Smart Grid, vol. 4, no. 3, pp. 1314-1322, Sept. 2013,

[9] A. Orcajo, Gonzalo; R. Díez, Josué; Cano, José M.; G. Norniella, Joaquín; Pedrayes G. J. Francisco; Rojas G., Carlos. “Coordinated Management of Electrical Energy in a Hot Rolling Mill and a Wind Farm”. 2021 IEEE Industry Applications Society Annual Meeting (IAS Meeting), pp. 1-9. Vancouver, Canada, Oct 2021. DOI: pending (to be published in IEEE Xplore Digital Library).

[10] T. Ding, S. Liu, W. Yuan, Z. Bie and B. Zeng, "A Two-Stage Robust Reactive Power Optimization Considering Uncertain Wind Power Integration in Active Distribution Networks," in IEEE Transactions on Sustainable Energy, vol. 7, no. 1, pp. 301-311, Jan. 2016, doi: 10.1109/TSTE.2015.2494587.

[11] O. Alsac, J. Bright, M. Prais, and B. Stott, “Further developments in Lp-based optimal power flow,” IEEE Trans. Power Syst., vol. 5, no. 3, pp. 697–711, Aug. 1990.

[12] M. B. Liu, S. K. Tso, and Y. Cheng, “An extended nonlinear primal-dual interior-point algorithm for reactive-power optimization of large-scale power systems with discrete control variables,” IEEE Trans. Power Syst., vol. 17, no. 4, pp. 982–991, Nov. 2002.

[13] J. Z. Zhu, C. S. Chang, W. Yan and G. Y. Xu. "Reactive power optimization using an analytic hierarchical process and a nonlinear optimization neural network approach", IEE Proc. Generation, Transmission, and Distribution, vol. 145, pp. 89-97, 1998.

[14] K. Iba, “Reactive power optimization by genetic algorithm,” *IEEE Trans. Power Syst.*, vol. 9, no. 2, pp. 685–692, May 1994.

[15] S.H. Zanakis and J.R. Evans. Heuristics optimization: Why, When and How to use it. Interfaces, Vol. 11, no.5, Oct. 1981

[16] B. Zhao, C. X. Guo, and Y. J. Cao, “A multiagent-based particle swarm optimization approach for optimal reactive power dispatch,” IEEE Trans. Power Syst., vol. 20, no. 2, pp. 1070–1078, May 2005.

[17] H. Yoshida *et al.*, “A particle swarm optimization for reactive power and voltage control considering voltage security assessment,” *IEEE Trans. Power Syst.*, vol. 15, no. 4, pp. 1232–1239, Nov. 2000.

[18] D. Koraki and K. Strunz, "Wind and Solar Power Integration in Electricity Markets and Distribution Networks Through Service-Centric Virtual Power Plants," in IEEE Transactions on Power Systems, vol. 33, no. 1, pp. 473-485, Jan. 2018, doi: 10.1109/TPWRS.2017.2710481.

[19] G. A. Orcajo, J. Rodríguez D., P. Ardura G., J. M. Cano, J. G. Norniella, R. Llera T., D. Cifrián R. “Dynamic Estimation of Electrical Demand in Hot Rolling Mills” *IEEE Transactions on Industry Applications* vol. 52, nº 3, May/June 2016.

[20] Y. Zhang, E. Muljadi, D. Kosterev and M. Singh, "Wind Power Plant Model Validation Using Synchrophasor Measurements at the Point of Interconnection," in IEEE Transactions on Sustainable Energy, vol. 6, no. 3, pp. 984-992, July 2015, doi: 10.1109/TSTE.2014.2343794.

[21] R. Cardenas, R. Pena, S. Alepuz and G. Asher, "Overview of Control Systems for the Operation of DFIGs in Wind Energy Applications," in IEEE Transactions on Industrial Electronics, vol. 60, no. 7, pp. 2776-2798, July 2013, doi: 10.1109/TIE.2013.2243372.

[22] L. Yang, Z. Xu, J. Ostergaard, Z. Y. Dong and K. P. Wong, "Advanced Control Strategy of DFIG Wind Turbines for Power System Fault Ride Through," in IEEE Transactions on Power Systems, vol. 27, no. 2, pp. 713-722, May 2012, doi: 10.1109/TPWRS.2011.2174387.

[23] ArcelorMittal News. “Storm is building Belgium’s first subsidy-free wind farm at ArcelorMittal Belgium in Ghent”. https://belgium.arcelormittal.com/en/storm-is-building-belgiums-first-subsidy-free-wind-farm-on-the-grounds-of-arcelormittal-belgium-in-ghent/ (accessed Dec. 3, 2021).

[24] A. Giannitrapani, S. Paoletti, A. Vicino and D. Zarrilli, "Bidding Wind Energy Exploiting Wind Speed Forecasts," in IEEE Transactions on Power Systems, vol. 31, no. 4, pp. 2647-2656, July 2016, doi: 10.1109/TPWRS.2015.2477942.

[25] Jager, D.; Andreas, A.; (1996). NREL National Wind Technology Center (NWTC): M2 Tower; Boulder, Colorado (Data); NREL Report No. DA-5500-56489. Available at http://dx.doi.org/10.5439/1052222.

[26] R. Dones, T. Heck, S. Hirschberg, “Greenhouse Gas Emissions from Energy Systems, Comparison and Overview”. Encyclopedia of Energy, Elsevier. 2004, Pages 77-95

[27] Mónica Alonso M. PhD Thesis “Gestión óptima de potencia reactiva en sistemas eléctricos con generación eólica”. Carlos III University, 2010.

[28] T. Lund, P. Sorensen, J. Eek. “Reactive power capability of a wind turbine with doubly fed induction generator”. Wind Energy 2007; 10. 379-394

[29] Spanish Regulation. BOE-A-2014-6123 Real Decreto 413/2014. Available at https://www.boe.es/diario_boe/txt.php?id=BOE-A-2014-6123.

[30] Y. L. Chen and C. C. Liu. "Optimal multi-objective Var planning using an interactive satisfying method", IEEE Trans. Power Syst., vol. 10, pp. 664670, 1995

[31] Eghbal M., N. Yorino, El-Arabi E.E., Zoka Y. “Multi-load level reactive power planning considering slow and fast VAR devices by means of particle swarm optimization” IET gener. Transm. Distrib., 2008, Vol. 2, nº 5. pp 743-751

[32] Cano J. M, G. Norniella J., Rojas C., A. Orcajo G., Juri Jatskevich “Application of Loop Power Flow Controllers for Power Demand Optimization at Industrial Customer Sites”. 2015 IEEE Power & Energy Society General Meeting.

[33] MathWorks. The MathWorks—MATLAB and Simulink for Technical Computing. Available at http://www.mathworks.com.

[34] P. Hou, W. Hu, M. Soltani and Z. Chen, "Optimized Placement of Wind Turbines in Large-Scale Offshore Wind Farm Using Particle Swarm Optimization Algorithm," IEEE Transactions on Sustainable Energy, vol. 6, no. 4, pp. 1272-1282, Oct. 2015, doi: 10.1109/TSTE.2015.2429912.

[35] Bhaskar Kanna, Sri Niwas Singh, “Towards reactive power dispatch within a wind farm using hybrid PSO” Electrical Power and Energy Systems. 2015. 69.232-240.

[36] A. H. Khan et al., "Optimal Portfolio Management for Engineering Problems Using Nonconvex Cardinality Constraint: A Computing Perspective," in IEEE Access, vol. 8, pp. 57437-57450, 2020, doi: 10.1109/ACCESS.2020.2982195.